

https://dspace.org/

Digital computer solution of special electrostatic and elastostatic problems with applications to the mining of tabular deposits

2015-02-09
http://hdl.handle.net/10539/16950

Downloaded from a DSpace repository. https://dspace.org/

The latter conditions establish the continuity of displacements in the mined area, where $S_z(x,y)$ is the vertical closure, and $s_x(x,y)$ & $s_y(x,y)$ are ride components (i.e. relative horizontal displacements of points vertically above each other on the roof and the floor.)

The boundary conditions (equations 2.1 and 2.2) together with the general equations of the model (Appendix 1) and the mining geometry, define the problem. Analytic solutions can be found only for a very limited number of geometries, e.g. an infinitely long rectangular panel or circular excavation. Thus a numerical approach is necessary.

2.1.2 Elemental Description

Since irregularly shaped excavations will have to be described in numerical terms, it is proposed to approximate the area by means of a regular mesh. The shape of the mesh elements will be chosen as square. Ideally, the elements would be infinitesimal.

2.1.3 Kernel Functions and Green's Functions as Solutions

The proposed method of solution is based on integral equations of the following form :-

$$\text{Effect at } (x,y,z) = \int_A K(x,y,z;\ \xi,\ \eta,\ \zeta)\ A(\xi,\ \eta,\ \zeta)\ d\xi\ d\eta\ d\zeta$$

where the integral is taken in general over all surfaces bounding the medium.

Here $A(\xi,\eta,\zeta)$ is interpreted as a density function to be defined on a boundary surface. Kernels, $K(x,y,z;\ \xi,\ \eta,\ \zeta)$ sometimes called influence functions, identically satisfy the elastic laws. In the special case of flat reefs at infinite depth these obey Laplace's Equation, in which case the kernels take the form of Green's functions.

Bateman[15] suggests that the solution of a problem, in which a solution of Laplace's equation is to be determined from a knowledge of its behaviour at certain boundaries, can be made to depend on that of another problem - the determination of the appropriate Green's function. This function has the following properties :-

(1) $\nabla^2 G = 0$, i.e. $G(P,Q)$ is a solution of Laplace's equation.

(ii) It is finite and continuous (differentiable to the second order with respect to x,y,z in general co-ordinates at any point, P, and also with respect to ξ, η, ζ at a particular point, Q), in space in a region bounded by a surface, S, except in the neighbourhood of the point, Q, where it is infinite; for example $\frac{1}{R}\cos(kR)$, $R \to o$, R being the distance between P and Q.

(iii) At the surface, S, some boundary conditions, such as $G = 0$ (Dirichlet Problem) or $\frac{\partial G}{\partial n}$ (Neumann problem), where $\frac{\partial}{\partial n}$ denotes the normal derivative, are satisfied.

It is also shown that Green's function as a solution of Laplace's equation, when it exists, is unique.

2.2 Qualitative Development of the Numerical Technique

The starting point in the development of a method is with the non-zero boundary condition, i.e. $\sigma_z = - q_z$ in the open mined region. Imagine this stress imposed on each of the elements of this area, i.e. imposing forces $F_z = \sigma_z \Delta A$; consider a line of symmetry passing through the middle of the reef plane as shown in Figure 2.2. Henceforth only one half plane need be considered, since, as stated earlier, there is symmetry above and below this line.

Consider now the forces exerted on one element in the positive half-space (z +ve downwards) (Figure 2.3 a); that element will be displaced, and neighbouring elements will also be displaced, as illustrated in Figure 2.3 b; since the forces are exerted on each

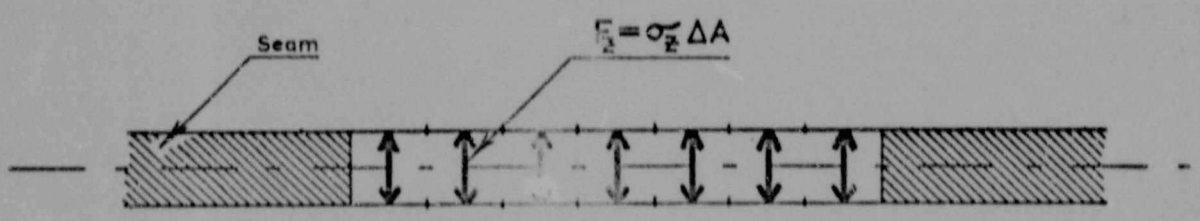

Figure 2.2 Forces Exerted on Elements in the Mined Area



Figure 2.3 a
Force Applied on 1 Element

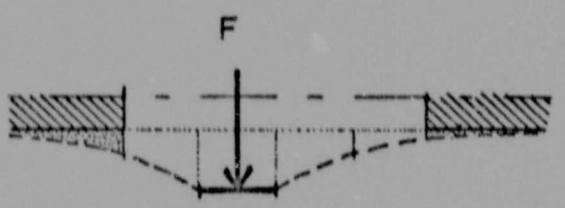

Figure 2.3 b
Deformation of Floor due to Force

element, independent of its neighbour, the resultant displacement is the sum of the individual displacements (Figure 2.4)

Ideally there would be displacements in the mined areas and zero displacements in the intact areas; then the resultant displacements in the mined areas would be the solution to the problem; however, such an effect cannot exist since physically this would imply a discontinuity in the medium above and below the plane of symmetry at the border of the mined-intact regions.

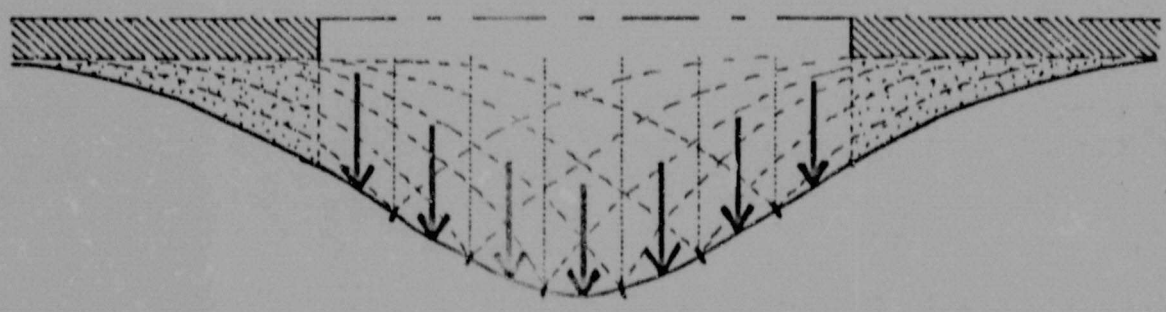

Figure 2.4 Cumulative Deformation Effect due to Forces on all Elements

Thus, as implied in Figure 2.4, the influences predict some distribution of displacements in the intact areas. But these displacements do not physically exist, as they would imply a parting of the seam along the plane of symmetry; hence one must apply an equal and opposite displacement distribution in the intact areas, restoring the displacements back to zero (Figure 2.5)

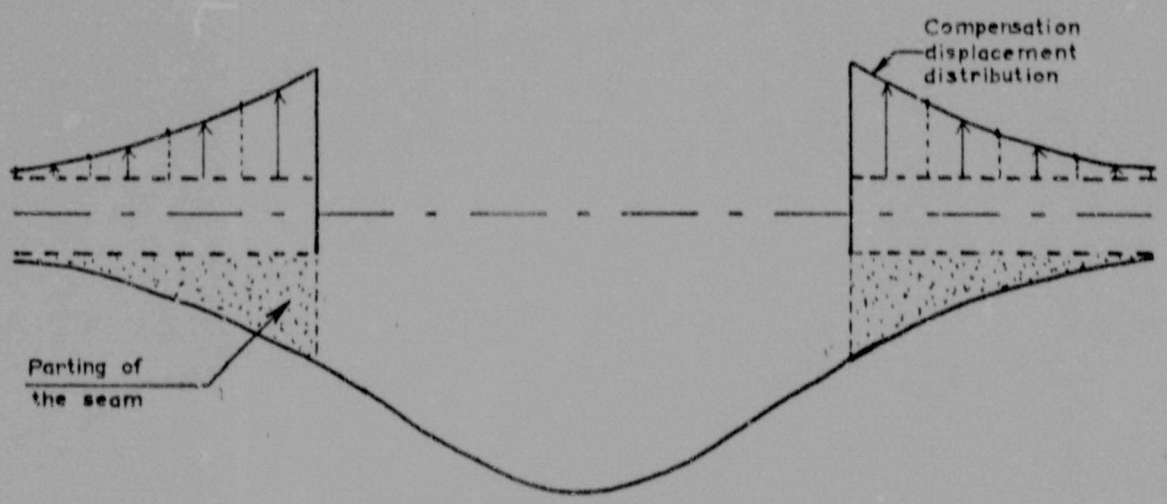

Figure 2.5 Imaginary Displacement Distribution in the Seam

This implies displacing each element in the intact area back to zero. Each elemental displacement is applied individually independent of the displacements of its neighbours (Figures 2.6 a and b). But these displacements cause stresses, distributing everywhere in the medium, as each causes the rock to move, resulting in a compressive stress above the element and an influence field of tensile stresses in the surrounding medium.

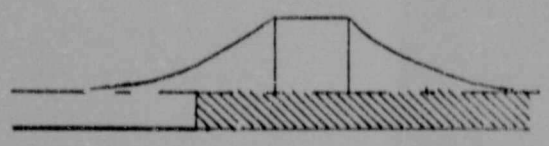

Figure 2.6 a
Displacement Imposed on an Element

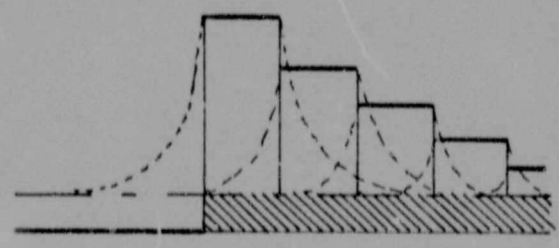

Figure 2.6 b
Displacements & the Stress Distributions Caused (dotted)

As was the case with the displacements in the intact areas, equal and opposite effects of stresses must be applied to the elements to restore the overall effect in the mined region to the known boundary conditions. If the change in imposed effects is smaller than the originally applied forces, F_z, and the method iterated back and forth in the manner described above, then there will be a convergence to a solution.

The solution after iterating to a sufficient accuracy will be of the form :-

In the mined region for each element

Boundary conditions = $-q_z$ = compensation effect + mined - to - intact effect

In the intact region for each element

Boundary conditions = 0 = compensation displacement + intact - to - mined effect

Quantitative expressions will be developed later. Thus the solutions are induced compensation stresses in the mined region and induced compensation displacements in the intact region. Making use of the influence functions once more to the stresses in the

mined area, a displacement distribution known as a convergence is obtained for the roof and floor, i.e. S_z. Using the influence functions on the displacements in the intact area, an induced stress distribution is obtained in that region, which, together with the primitive stresses, allows the calculation of the resultant stresses in the intact areas.

This is then the desired solution on the reef plane and Salamon[6] shows that, knowing these distributions, the stresses and displacements may be calculated at any point in the medium by the use of suitable influence functions.

2.3 The Choice of Green's Function

The problem is now considered in quantitative terms. Consider the analogy with an electrostatic system where the potentials (V) correspond to the stresses. Then a function which comes to mind is one relating the potential (V) at a point to an electrostatic charge or an electric field (E). This function is[21]:

$$V = \frac{1}{2\pi} \frac{1}{\sqrt{r^2 + z^2}} E_a \Delta A \quad \text{(E - function)} \qquad \ldots\ldots\ldots\ldots(2.3)$$

where $r = \sqrt{x^2 + y^2}$ (cylindrical co-ordinate), and field E has a value E_a at the particular elemental area ΔA.

As shown in Appendix II.1, this function satisfies the properties of a Green's function as laid down in §2.1.3; thus it allows the potential, V, to be calculated at a remote point (x,y,z), due to the presence of a known electric field, E, at an elemental area at relative co-ordinates (0,0,0).

Consider the special case of application of this function on the z = o plane; then 2.3 becomes :

$$V = \frac{1}{2\pi r} E_a \Delta A \qquad \ldots\ldots\ldots\ldots\ldots\ldots\ldots\ldots\ldots\ldots(2.4)$$

Using the analogous properties, this allows the displacements in the intact area, as a result of a stress on an element ΔA, to be calculated. This function is singular at $r \to 0$, but, if considered to be averaged over the area ΔA, then, from Appendix II.1 equation (II.5), the following relation holds :

$$V = \frac{4}{\pi} \ell n (1 + \sqrt{2}) E_a \Delta A = 0,561099\ E_a \Delta A \quad \ldots\ldots\ldots\ldots\ldots\ldots (2.5)$$

How does this function relate to other normal stresses in the open mined area?

Now,

$$E_n = \left(- \frac{\partial V}{\partial z} \right)_{z=o} \quad \ldots\ldots\ldots\ldots\ldots\ldots\ldots\ldots\ldots\ldots\ldots\ldots\ldots\ldots (2.6)$$

Differentiating equation 2.3

$$E_n = \frac{1}{2\pi} \frac{z}{(r^2 + z^2)^{3/2}} E_a \Delta A \quad \text{with } z=o \quad \ldots\ldots\ldots\ldots\ldots\ldots\ldots (2.7)$$

Thus,

$$(E_n)_{z=o} = 0 \quad \ldots\ldots\ldots\ldots\ldots\ldots\ldots\ldots\ldots\ldots\ldots\ldots\ldots\ldots (2.8)$$

The equation (2.7) has the desired properties (§2.2) of no effects to the stresses on other mined elements (on the z=o plane) due to the application of a stress to a particular element.

Now another function is required. The desired properties from §2.2 are that, for a displacement specified on an element in the intact area, this should have no effect on other elements in the intact area (on the z=o plane), but should cause a stress effect on the mined elements in the same plane. Equation 2.7 gives the clue to the form of influence function which would satisfy these properties. Thus the following is suggested :-

$$V = \frac{z}{2\pi\ (r^2 + z^2)^{3/2}} V_a \Delta A \quad \text{(V-function)} \quad \ldots\ldots\ldots\ldots (2.9)$$

The function

$\frac{z}{2\pi\ (r^2 + z^2)^{3/2}}$ is shown in Appendix II.2 to be a Green's function.

Also

$$(V)_{z=o} = 0$$

Thus the normal fi $E_n = \left(- \frac{\partial V}{\partial z} \right)$ from this function is

$$E_n = -\left(\frac{1}{2\pi\ (r^2 + z^2)^{3/2}} \right) - \frac{3z^2}{2\pi\ (r^2 + z^2)^{5/2}} V_a \Delta A \quad \ldots\ldots\ldots (2.10)$$

Thus for the z=o plane

$$(E_n)_{z=o} = -\frac{1}{2\pi r^3} V_a \Delta A \qquad \text{.....(2.11)}$$

which is singular for $r \to o$, but, if $r \to o$ implies averaging over the finite element ΔA, then

$$(E_n)_{z=o,\ r=o} = \frac{8}{\sqrt{2}\,\pi} V_a \Delta A = 1{,}800633\ V_a \Delta A \qquad \text{.....(2.12)}$$

2.4 Conclusions

Note that the development here has outlined one approach that has resulted in a well-behaved set of kernels. Using the ideas of the qualitative approach to the problem in §2.2, and the quantitative relationships of §2.3, an inherently fast converging method has been developed. The details are studied in the next chapter.

CHAPTER 3

FEASIBILITY TESTS

3.1 Initial Test

Feasibility tests were carried out using a Fortran program. This was done in order to establish whether the method as described in § 2.3, would give satisfactory results. The latter was judged by closeness to the theoretical solutions for some standard excavation shapes. The flowchart for this program, together with its listing and printout of some sample runs, is given in Appendix IV.

Certain techniques which were used in this program in order to speed up the calculation were used again in the final implementation of the system in what will be called MINSIM in Chapter 4. These features are introduced in the sections that follow.

3.1.1 Iterative Techniques

The method as described in § 2.2 is developed below in an iterative form. As was mentioned earlier, the initial ideas were developed in terms of electric fields, E, and potentials, V, all on the z = o plane.

Let the effects of the applied fields E upon the potentials in the intact area be

$$\bar{V} = K_1 E_i \qquad \text{.....(3.1)}$$

where i is the iteration count.

$E_o = E_b$	the boundary conditions for E
E_i is an (n x 1)	vector of mined fields
$\bar{V}$ is an (m x 1)	vector of intact potentials
K_1 is an (m x n)	matrix

of the form $\frac{1}{2\pi r} = \frac{1}{2\pi\sqrt{x^2 + y^2}}$, when evaluated on the appropriate square-to-point distances.

Similarly, the V to E effect may be written as

$$\bar{E} = K_2 V_i \qquad \text{.....(3.2)}$$

where K_2 is an (n x m) matrix, which for the z = o plane, is of the form $-\frac{1}{2\pi r^3} = -\frac{1}{2\pi (x^2 + y^2)^{3/2}}$, when evaluated on the appropriate square-to-point distances. Then, in order to satisfy the boundary conditions,

$$V_b = V_{i+1} + \bar{V} = V_{i+1} + K_1 E_i \qquad \text{.....(3.3a)}$$

and

$$E_b = E_{i+1} + \bar{E} = E_{i+1} + K_2 V_{i+1} \qquad \text{.....(3.3b)}$$

and, in a more useful form for performing the iterating,

$$V_{i+1} = V_b - K_1 E_i \qquad \text{.....(3.4a)}$$

$$E_{i+1} = E_b - K_2 V_{i+1} \qquad \text{.....(3.4b)}$$

where $V_b = 0$

and $E_b = -q_z$ } ...(3.5)

If the solution converges, then, applying a suitable convergence criterion such as

$$\text{Maximum}_{(\text{mined elements})} \left| \frac{E_{i+1} - E_i}{E_{i+1}} \right| < \varepsilon \qquad \text{.....(3.6)}$$

the solution is stopped after, say, k iterations. Then E_k and V_k are regarded as internal solutions, as they give the induced potentials in the intact area and induced fields in the mined area. Thus one more integration is performed to obtain potentials, corresponding to displacements in the mined area due to the induced fields in that area. Fields corresponding to stresses, in the intact area due to the induced potentials there, were not initially of interest in the tests.

Use is made of equation (3.1) for the effects of points surrounding the square of interest and the self-effects from equation (2.5) which is :

$$V_{(x,y,z = o)} = 0,561100\ E = \frac{2}{\pi} \ln(1 + \sqrt{2})\ E$$

3.1.2 Features of the Test Program

3.1.2.1 Kernel Calculations

The kernels - K_1 and K_2 - used on the z = o plane are functions of r only, where r is the distance of the from-points, (the squares affecting the square in question), to the to-point, (the square affected). It is obvious, as illustrated in Figure 3.1, that the same kernel will be used for many calculations of square-to-point effects (e.g. for squares 1, 2, 3, 4, 5 in Figure 3.1), and, when the calculation moves to the next to-point again the same kernels might be used. Thus the best strategy is to calculate one set of kernels as functions of distance; these are kept in a table and referred to when needed without re-calculation.

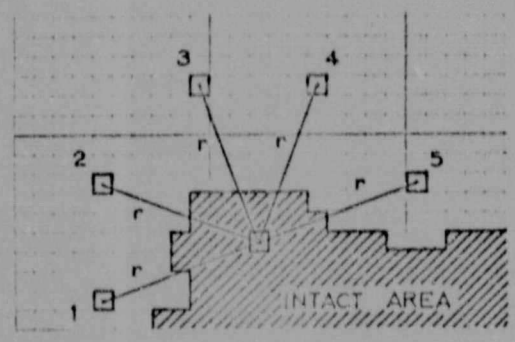

Figure 3.1 Equidistant Points

Certain symmetries were evident when using a square mesh. Consider the situation as illustrated in Figure 3.2. It is seen that, since $r = \sqrt{x^2 + y^2}$, there are eight squares equidistant from a central point. Thus it is only necessary to calculate kernels for a triangular area as shown in Figure 3.3.

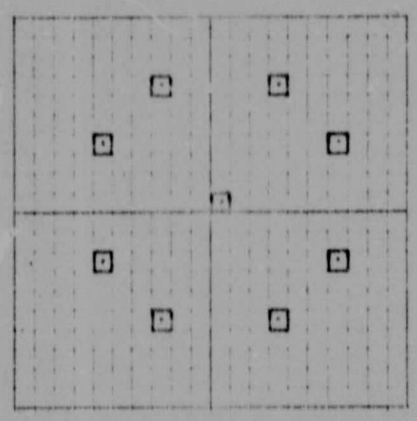

Figure 3.2 Equidistant Points

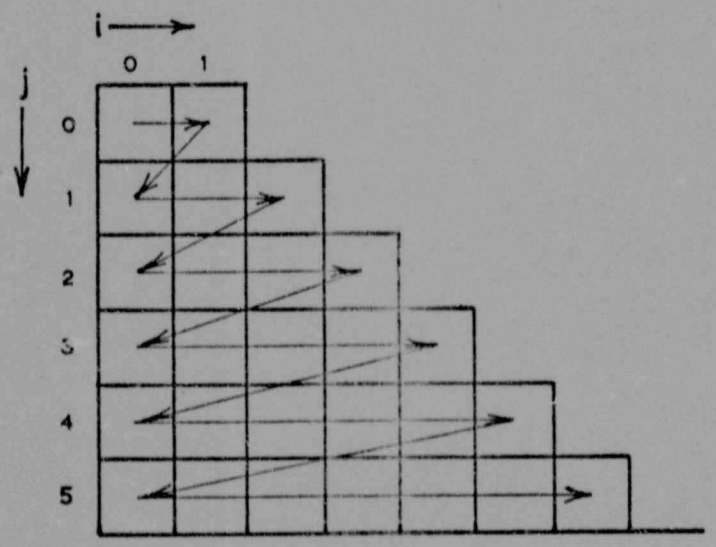

Figure 3.3 Order of Storage

This method was used in the feasibility program given in Appendix IV. The kernel elements were stored in a linear array in an order as shown by the arrows. Finding the value of a particular kernel involved calculating the linear offset according to the algorithm :-

Let i = lesser of x and y
j = greater of x and y
then offset = j(j + 1)/2 + i .....(3.7)

This involves an integer multiplication, division, and two additions and editorial overheads which on the IBM 360/50 computer, takes a total CPU time of 98,88 μs (see Appendix V). If the kernels were calculated each time this would involve two floating-point multiplies, one floating point divide and a branching to the SQRT function. The CPU time in this case would be approximately 560 μs. The benefits of using a table are thus obvious.

3.1.2.2 Input and Output Communications

The program was designed to accept any excavation shape as quantized on to a maximum mesh of 60 x 60 squares. As calculated later, § 3.1.4, a full-size 60 x 60 plan would not be computable within any reasonable time.

The input was on cards occupying columns 1 to 60 as a maximum. The intact area was represented by zero's or blanks, and the mined area by ones. A picture of the input was printed as shown as an example in Figure 3.4 with x's representing the intact areas and blanks in the mined area.

```
.XXXXXXXXXXX
.XXXXXXXXXXX
.XXXXXXXXXXX
.XXX      XXX
.XXX      XXX
.XXX      XXX
.XXX      XXX
.XXX      XXX
.XXXXXXXXXXX
.XXXXXXXXXXX
.XXXXXXXXXXX
```

Figure 3.4 Example of Input

Initially, in order to observe the values of the tables of each iteration, printout of the whole solution table E was performed. At convergence of the solution the potentials in the mined area were calculated and printed.

The problem was normalised - unit squares, and boundary conditions in the mined area = 1. In the intact area the boundary conditions are zero.

3.1.3 Results

The excavation shape as illustrated in Figure 3.4 was supplied to the program.

No analytic expressions could be found in the literature for a square excavation. The results of this experiment were observed therefore for their qualitative nature.

The results, given fully in Appendix IV, exhibit the expected symmetries, and all the information is shown in Figure 3.5 and displayed graphically in Figure 3.6, with traverses across the two sections XX and YY.

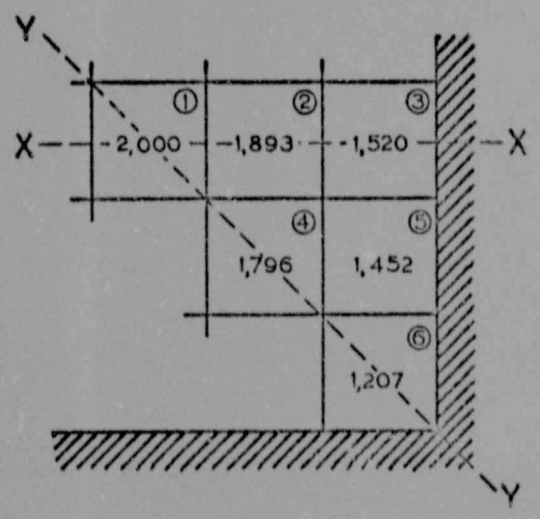

Figure 3.5 Results

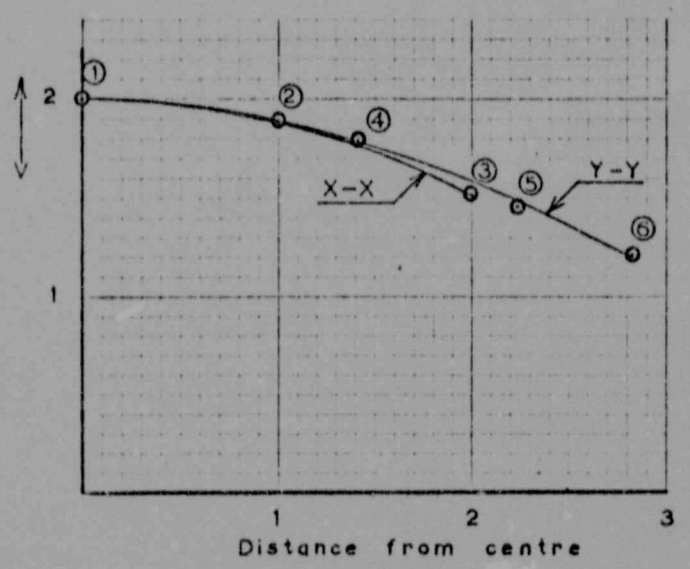

Figure 3.6 Graph of T[illegible]erses X-X and Y Y

From the graph it may be seen that the general shape of the potentials is as expected. At the edges, in the intact area, the potentials should be zero. Smooth curves can be extrapolated from the results, although there is no justification for doing so apart from the knowledge of the boundary conditions.

3.1.4 Computer (CPU) Timings

As indicated by comments in the program of Appendix IV, a timing program available at the University of the Witwatersrand Computing Centre was used and yielded the results as shown in Appendix IV.5.

Hence, it may be seen that, using the IBM FORTRAN H compiler on the 360/50, the time taken per complete iteration loop was 4,3 seconds. This is for the current problem of 11 x 11 squares, i.e. 121 points, of which 25 were mined. This calculation involved 96 calculations of the effects of 25 points and 25 calculations of the effects of 96 points, i.e. 2 x 96 x 25 = 4 800 calculations. (The worst case would be for an equal number of mined and intact points, i.e. 60 x 61 x 2 = 7 320 calculations).

Now it is intended eventually to solve a problem having a maximum of about 60 x 60 mesh. This would involve 2 x ($\frac{1}{2}$ x 60 x 60) i.e. 6 480 000 calculations. Using the current program, this would take a total computing time of $\frac{6\ 480\ 000}{4\ 800} \times 3{,}8 \times \frac{1}{60} \times \frac{1}{60} = 1{,}6$ hours.

This is the present solution of a simple shape, the only point varying most per iteration being the corner of the excavation. Yet it needed 14 iterative loops to find a solution of the required accuracy. If, however, the accuracy level is dropped so as to need only 10 iterations to achieve a solution, this could take of the order of 16 hours.

Obviously, therefore, the present program is impractical from a time point of view, and ways of speeding up the solution must be sought.

3.2 Modifications to the First Program

Consider the problem illustrated in Figure 3.7. Let the calculations of V proceed as before but, for the first few iterations, only as far into the intact area as the layer indicated by the check lines, and, gradually increasing the width of this influence layer, until the full area is taken into account. It was hoped that the solution would have almost converged by that time. Then, because less elements are considered initially, the first few iterations will be much faster.

The justification for this method of iterating is in the form of the kernel functions, viz. $\propto \frac{1}{r}$ and $\propto \frac{1}{r^3}$ respectively, i.e. a fairly rapid fall off in influence with distance. The results, as may be seen from Appendix VI, agree with the first program results to the 4th and, in some cases, the 5th significant digit. In addition, only

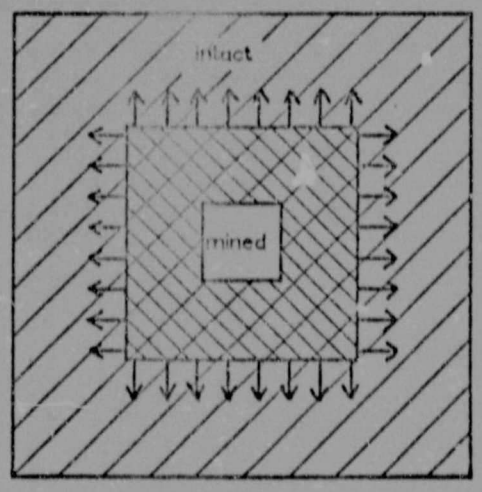

Figure 3.7 Expanding Regions of Influence

12 iteration loops were needed, as opposed to 14 in the first case, for the same accuracy criterion of the 0,1% change.

When the error criterion was dropped to 1%, only 6 iteration loops were required and the results agreed with previous results to better than 1%.

3.3 Some Further Tests

3.3.1 A Parallel Slit

A parallel slit of 5 x 11 in an 11 x 11 area was solved. A graph of the results (see Appendix VI) is shown in Figure 3,8, with the theoretical and infinite parallel slit drawn in for comparison (ref. Appendix III). Comparing the cross-sectional traverses YY and XX, it is seen that the results approach the theoretical curves taken for slit widths 5 and 6. Of course the problem suffers from the "edge effect", i.e. the borders of the problem are relatively close to the cross-traverse of interest. In fact the problem is a very crude approximation to the infinite parallel slit, its length being only 2,2 x its width.

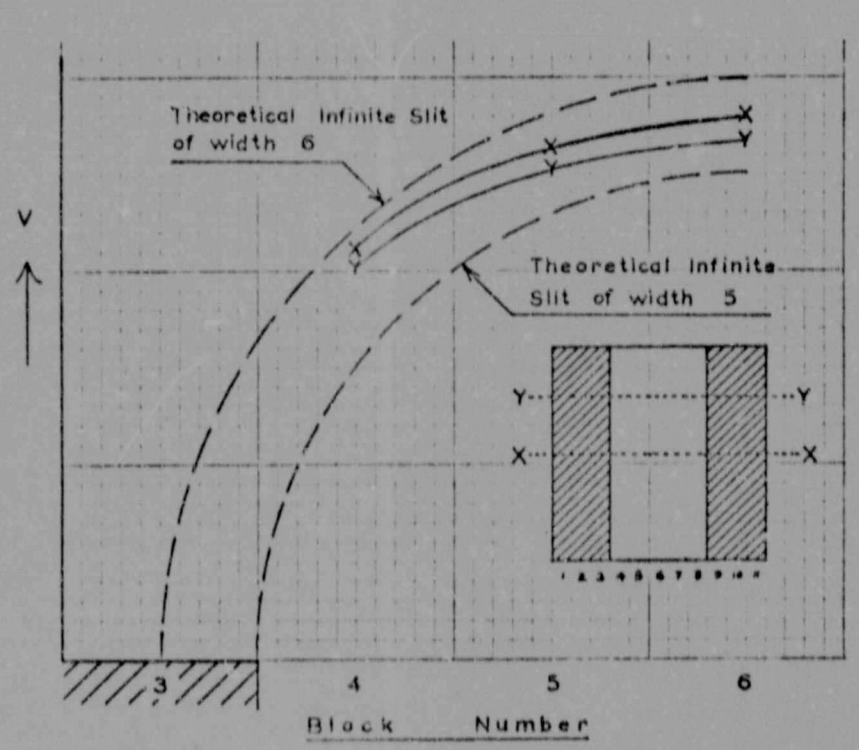

Figure 3,8 A Parallel Slit

3.3.2 A Circular Excavation

3.3.2.1 First Attempt

A 21 x 21 element plan was considered with a crude approximation to a 15 unit diameter circular excavation as illustrated in Figure 3.9. This was the first example which posed a real difficulty in solution. Fortunately the tests were performed at a time when ample computer time was available.

This problem eventually converged to a solution after 75 iterations in approximately 3 hours. This situation will be examined further in the next section.

Table 3.1 below, shows the results of traverses x-x, and y-y (see Figure 3.9). (Further results appear in Appendix VI).

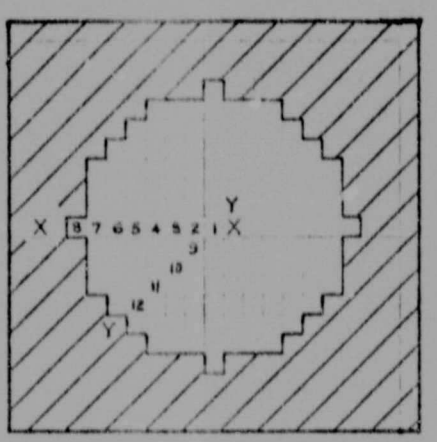

Figure 3.9 Circular Excavation

Using the analytic solution for a circular excavation (ref. Appendix III) and the centre potential results, an effective radius was calculated from

$$4,7796 = \frac{2}{\pi} \sqrt{R^2 - 0}$$

$$\therefore \quad R = 7,508.$$

The theoretical results are added for comparison in table 3.1, and a graphical comparison may be seen in Figure 3.10.

As seen from the graph, there is close agreement towards the centre of the excavation.

Table 3.1 Two Traverses of 15 diameter Circular Excavation

Traverse XX				Traverse YY			
Point	Result	Theoretical	Error	Point	Result	Theoretical	Error
1	4,7796	4,7796	-	1	4,7796	4,7796	-
2	4,7340	4,7370	0,06%				
3	4,5945	4,6069	0,27%	9	4,6879	4,6940	0,13%
4	4,3520	4,3814	0,68%				
5	3,9877	4,0448	1,43%	10	4,4010	4,4274	0,60%
6	3,4652	3,5654	2,90%				
7	2,7388	2,8730	4,90%	11	3,8741	3,9433	1,78%
8	1,8722	1,7279	7,71%	12	2,9859	3,1425	5,25%

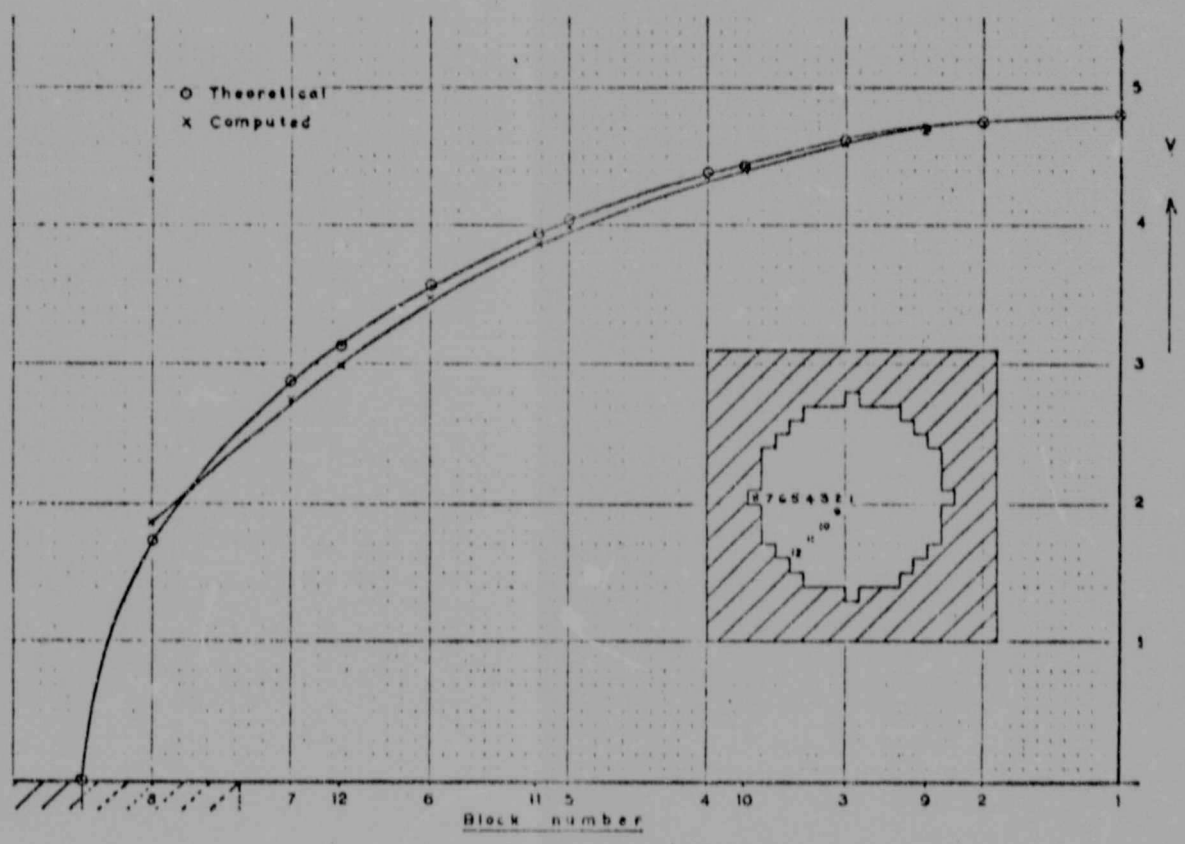

Figure 3.10 Graphical Results of 15 diameter Circular Excavations

Towards the edges of the excavation there is a steady decrease in the agreement, probably caused by the fact that the intact border is only 3 to 7 units in width and thus does not simulate a circular excavatio with no other effects close by.

Taking this into consideration, the agreement is good, and this feasibility test shows that the iterative method developed gives satisfactory results.

3.3.2.2 Second Attempt

The same circular excavation was solved using a 31 x 31 element plan so as to compare the effect of the rim of intact material round the borders. Full results will be found in Appendix VI.

Performing the same analysis as before, the effective radius of the circle is :

$$R = \frac{\pi}{2} \times 4,6316$$

$$= 7,275$$

This is a better fit to the diagram than before.

The results of an XX and YY traverse, together with theoretical results, are given in table 3.2 and a graphical comparison may be seen in Figure 3.11.

Table 3.2 Two Traverses of a Circular Excavation (larger rim)

Traverse XX				Traverse YY			
Point	Result	Theoretical	Error	Point	Result	Theoretical	Error
1	4,6316	4,6316	-	1	4,6316	4,6316	-
2	4,5866	4,5876	0,02%	9	4,5412	4,5432	0,05%
3	4,4497	4,4532	0,09%	10	4,2590	4,2672	0,19%
4	4,2103	4,2195	0,22%	11	3,7427	3,7625	0,53%
5	3,8521	3,8687	0,43%	12	2,8778	2,9125	1,21%
6	3,3399	3,3645	0,73%				
7	2,6311	2,6194	-0,44%				
8	1,7901	1,2620	-29 %				

Since the error criterion was a maximum of 1% change per iteration on a point, the results agree with the theoretical ones extremely well, the only point of gross error being point 8, which in any case juts out from the circle, and the result is probably correct. (There is less displacement here because of intact areas surrounding that element on 3 sides).

3.3.3 Two Circular Excavations

Two circular excavations of diameter approximating 10 units are positioned as shown in Figure 3.12 in a 31 x 31 element area. A graph is plotted (Figure 3.13) of the traverse XX (full results are given in Appendix VI). On the graph is shown the theoretical responses for each circular excavation as if the other did not exist, and the response of a circular excavation of diameter AA. The only conclusion that can be made is that the results are reasonable, as they fall between the two theoretical conditions.

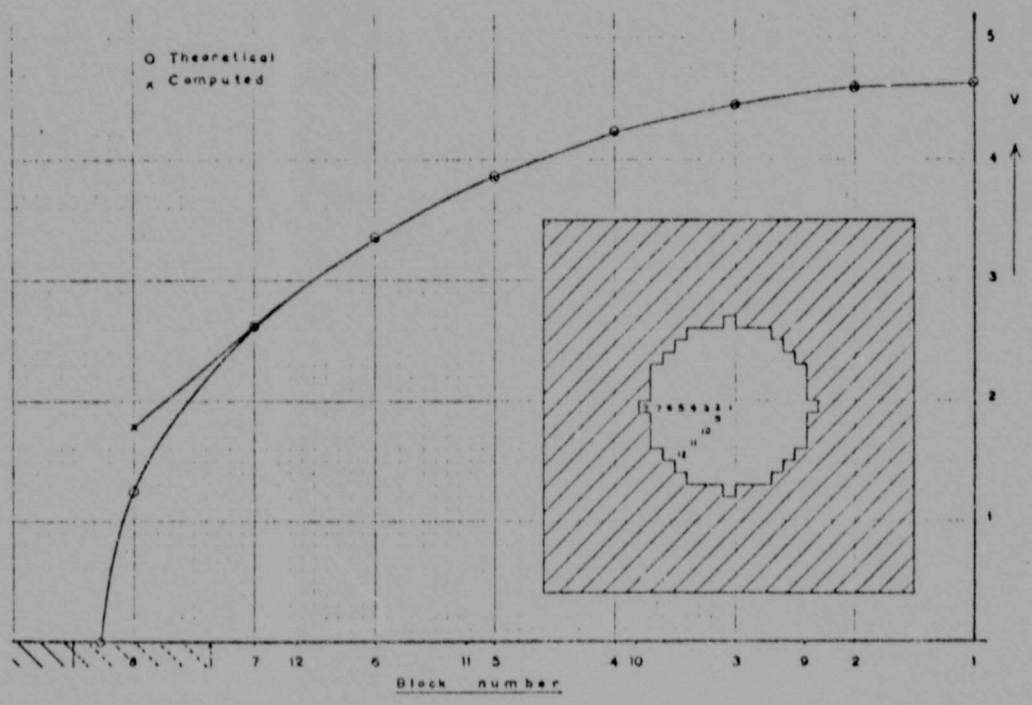

Figure 3.11 ~15 Diameter Circular Excavation (Target contact rim)

Author Cohen B
Name of thesis Digital computer solution of special electrostatic and elastostatic problems with applications to the mining of tabular deposits 1975

PUBLISHER:
University of the Witwatersrand, Johannesburg
©2013

LEGAL NOTICES:

Copyright Notice: All materials on the University of the Witwatersrand, Johannesburg Library website are protected by South African copyright law and may not be distributed, transmitted, displayed, or otherwise published in any format, without the prior written permission of the copyright owner.

Disclaimer and Terms of Use: Provided that you maintain all copyright and other notices contained therein, you may download material (one machine readable copy and one print copy per page) for your personal and/or educational non-commercial use only.

The University of the Witwatersrand, Johannesburg, is not responsible for any errors or omissions and excludes any and all liability for any errors in or omissions from the information on the Library website.